ELSEVIER

Catalysis Today 49 (1999) 267–276

CATALYSIS TODAY

Synthesis, characterization and catalytic properties of ZrAPO-5

M.K. Dongare*, D.P. Sabde, R.A. Shaikh, K.R. Kamble, S.G. Hegde

Catalysis Division, National Chemical Laboratory, Pune 411 008, India

Abstract

$AlPO_4$-5 and ZrAPO-5 molecular sieves were synthesized hydrothermally and characterized by XRD, SEM, MASNMR, FTIR, adsorption studies and TPD of ammonia. The results indicated that Zr was isomorphously substituted in the $AlPO_4$-5 structure. Increase in Brönsted and Lewis acidity was observed which resulted in increased activity and stability in *m*-xylene isomerization reaction.

Keywords: $AlPO_4$-5; ZrAPO-5; FTIR; TPD of ammonia; *m*-Xylene isomerization

1. Introduction

Zirconia in its pure and modified form is an important material as catalyst and catalyst support [1,2], but owing to the difficulty in preparation as highly dispersed state with high surface area, it has limited industrial applications. Among numerous studies devoted to this problem, those on zirconium containing microporous zeolites and mesoporous silicas are important. Despite some information available in patent literature [3,4], we have earlier reported the studies on the synthesis and characterization of zirconium containing silicalite-1 [5]. Later studies by others [6–8] further demonstrated that Zr^{4+} cation can be isomorphously substituted for Si^{4+} in high silica zeolites and mesoporous silicas; and has catalytic oxidation properties similar to well-known Ti incorporated molecular sieves. Catalytic activity of ZrO_2 can also be enhanced by promoting with sulphate anions (sulphated ZrO_2) [9,10], and by phosphate anions (phosphated ZrO_2) [11–16]. Whereas sulphated zirconia is nonporous, many examples of phosphated zirconia are microporous, mesoporous or lammellar materials having high surface area. While Ti containing $AlPO_4$- molecular sieves (TAPO-5 [17], TAPO-11 [17], TAPSO-5 [18]) are well documented, reports on zirconium containing $AlPO_4$- molecular sieves are not well established [14–16]. Nevertheless, it indicated that the presence of Zr in the catalyst enhances the life of the catalyst in reactions like skeletal isomerization of linear butenes [16] and isomerization of toluidines [19]. Therefore, we have studied the synthesis and physico-chemical properties of Zr incorporated $AlPO_4$-5 molecular sieves (ZrAPO-5). They were characterized by XRD, SEM, FTIR, MAS NMR, TPD of ammonia and catalytic activity in isomerization of *m*-xylene reaction.

2. Experimental

2.1. Synthesis

ZrAPO-5 with different Zr content were prepared from the gel compositions $1.5R : xZrO_2 : Al_2O_3 : -$

*Corresponding author.

0920-5861/99/$ – see front matter
PII: S0920-5861(98)00433-7

$P_2O_5 : 33H_2O$, where x was 0.04–0.08 and R was triethylamine (TEA). The source of Zr was not added in the gel to prepare pure $AlPO_4$-5 material. In a typical synthesis, 20.8 g of aluminium isopropoxide (98%, Aldrich) and 80 g of dry isopropyl alcohol (IPA) were mixed and stirred at 60°C for 1 h. Then 0.66 g zirconium propoxide (98%, Fluka) with 20 g of IPA was added slowly to the above mixture under vigorous stirring. Thorough mixing was continued for 45 min. The solution was warmed to 70°C for removing the IPA before adding 11.5 g orthophosphoric acid (85%, SD fine) with 30 g of water. After 1 h, 7.6 g TEA (99%, Ranbaxy) was added slowly and stirring was continued for another 1 h.

The composition of the precursor gel (for sample 2) was 0.04 $ZrO_2 : Al_2O_3 : P_2O_5 : 1.5TEA : 33H_2O$. The homogeneous gel was then transferred into a PTFE lined stainless steel autoclave and kept for crystallization at 200°C for 5 days. After crystallization, the white solid was recovered by filtration, washed several times with distilled water and dried in an oven at 100°C. The samples thus obtained were calcined in air to remove the template by heating slowly to 873 K and holding it for 8 h. The characterization of the samples was carried out by XRD (Rigaku, D-Max III VC Japan) with nickel filtered Cu K_α radiation. Sorption studies were carried out using all glass gravimetric apparatus with McBain–Baker type silica spring connected to a high vacuum system. For scanning electron micrograph (SEM), the sample powder was dispersed in ethyl alcohol for few seconds. A drop of this suspension was then placed as a thin film supported

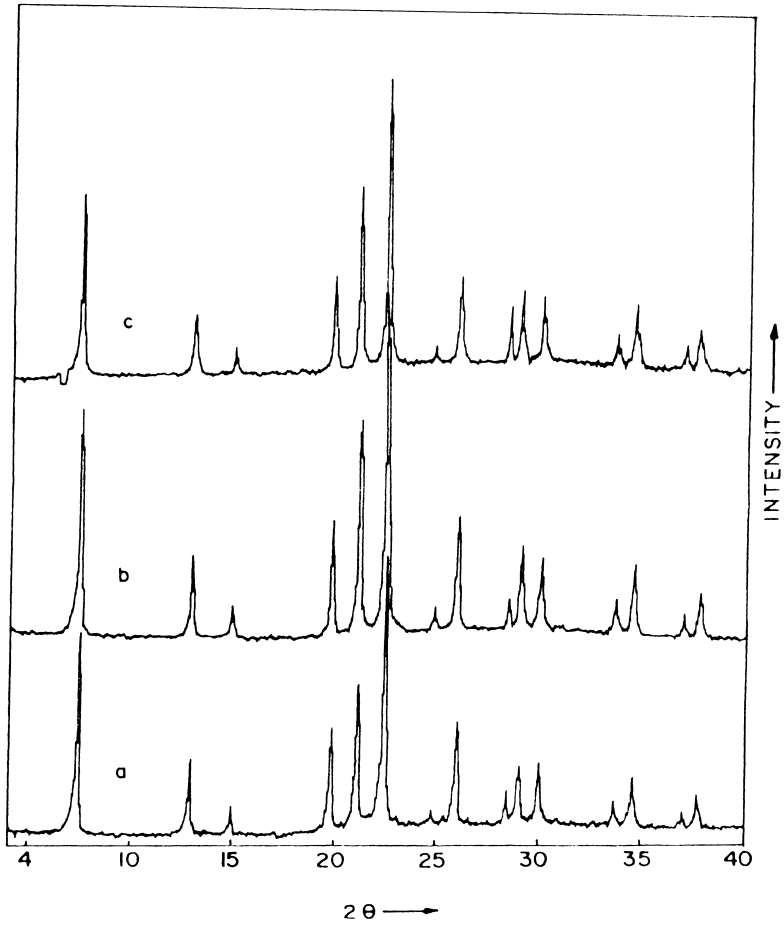

Fig. 1. XRD patterns of: (a) $AlPO_4$-5; (b) ZrAPO-5(0.04); (c) ZrAPO-5(0.08).

over specimen grid. The photographs were taken using Jeol JSM 500 electron microscope. The chemical composition of the sample was determined by XRF(Rigaku-3700) and the energy dispersive X-ray (EDX) analysis attached to SEM. FTIR spectra (1300–1400 cm^{-1}) was taken using KBr pellet technique, whereas self-supported wafer in a high temperature–high vacuum transmittance cell was used to study the nature of the surface hydroxyl groups (Nicolet,60 SXB spectrometer) as per the procedure [20] reported earlier. Solid state MASNMR spectrum was recorded using Bruker MSL 300 NMR spectrometer. The temperature programmed desorption (TPD) of NH_3 was done using Sorbstar (Model-200, Budapest). The catalytic experiments for *m*-xylene isomerization were performed in an all silica fixed bed vertical down flow reactor, taking 2 g of the catalyst particles of 10–20 mesh. Products were analyzed by gas chromatography (Shimadzu-15A) using xylene master capillary column with FID as a detector.

3. Results and discussion

XRD patterns of pure $AlPO_4$-5, ZrAPO-5 (0.04) and ZrAPO-5 (0.08) presented in Fig. 1(a)–(c) show that all samples have AFI ($AlPO_4$-5) topology and do not have any crystalline impurities. The chemical analysis and unit cell volumes of the samples are presented in Table 1. The increase in unit cell volume from 1366(Å) for pure $AlPO_4$-5 to 1372(Å) for ZrAlPO-5 (0.08) seems to be due to the Zr incorporation in the lattice. The chemical composition showed that the Zr content in the solid was always lower than in the reactive gel, and the Al/P+Zr ratio in the sample was near to 1. Therefore it seems that the substitution of Zr for only P in the lattice was predominant

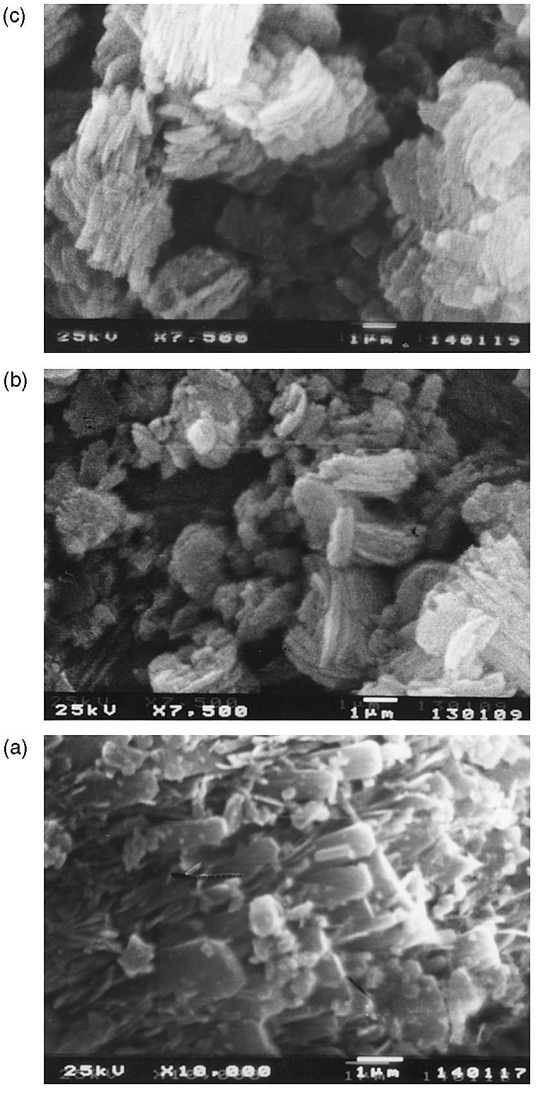

Fig. 2. SEM photographs of: (a) $AlPO_4$-5; (b) ZrAPO-5(0.04); (c) ZrAPO-5 (0.08).

Table 1
The physico-chemical characteristics of $AlPO_4$-5 and ZrAPO-5 samples

No.	Sample[a]	Composition of crystalline phase	BET surface area (m^2/gm)	Unit cell volume $(Å)^3$	Adsorption (wt%)	
					Water	Cyclohexane
1	$AlPO_4$-5	$Al_{2.0}P_{2.0}O_8$	395	1366.0	22.1	8.8
2	ZrAPO-5 (0.04)	$Al_{2.0}P_{1.97}Zr_{0.03}O_8$	340	1369.7	20.3	9.1
3	ZrAPO-5 (0.08)	$Al_{2.0}P_{1.94}Zr_{0.06}O_8$	342	1372.5	21.4	9.0

[a]No. in parenthesis indicates the ZrO_2 mole fraction in the reacting gel.

over the pairwise substitution of two Zr for Al+P cations.

SEM photographs (Fig. 2) showed that pure $AlPO_4$-5 crystallized in the form of hexagonal rods of irregular size, ranging from 0.5 to 3.0 μm. The morphology of ZrAPO-5 significantly changed depending on the Zr content. They consisted of bundles of needle like crystals with no sharp edges.

Adsorption properties of ZrAPO-5 samples are presented in Table 1. The equivalent BET surface area and the amount of H_2O and cyclohexane adsorbed were comparable to reported values [21]. These values showed that the materials were highly crystalline without any amorphous matter occluded in the pores. This is contrary to the findings of Meriaudean et al. [16], where in incorporation of Zr in SAPO-11 resulted in Zr species occluded in the pores. It should be noted that for ZrAPO-5 samples, N_2 adsorption was considerably less than that of $AlPO_4$-5, even though water and cyclohexane adsorption values were comparable. This is due to the difference in interaction of N_2 molecules with the surface. The possible reason [14] could be the condensation of N_2 around the zirconium centers, which could hinder and stop the diffusion and sorption of N_2. Thus it seems to indicate a framework incorporation of Zr ions in ZrAPO-5 samples.

The ^{31}P and ^{27}Al MASNMR spectra of calcined samples are presented in Fig. 3(a) and (b). The values of the chemical shift −30.8 ppm for ^{31}P and 36.78 ppm for ^{27}Al are typical of $AlPO_4$-5 structure reported [15,22]. There were no additional lines in the spectra, which indicated the absence of extra lattice P and Al species in the samples.

The FTIR spectra in the framework vibration region were recorded in the Fig. 4(a)–(c). Absorption bands

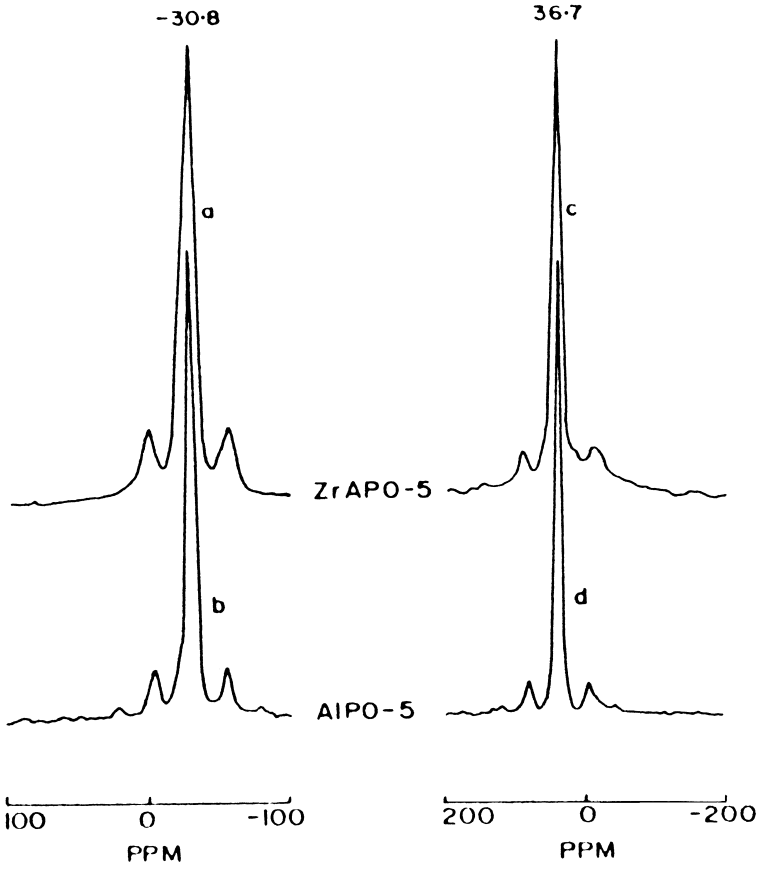

Fig. 3. ^{31}P (a,b) and ^{27}Al (c,d) MAS NMR spectra of $AlPO_4$-5 (b,d) and ZrAPO-5 (a,c).

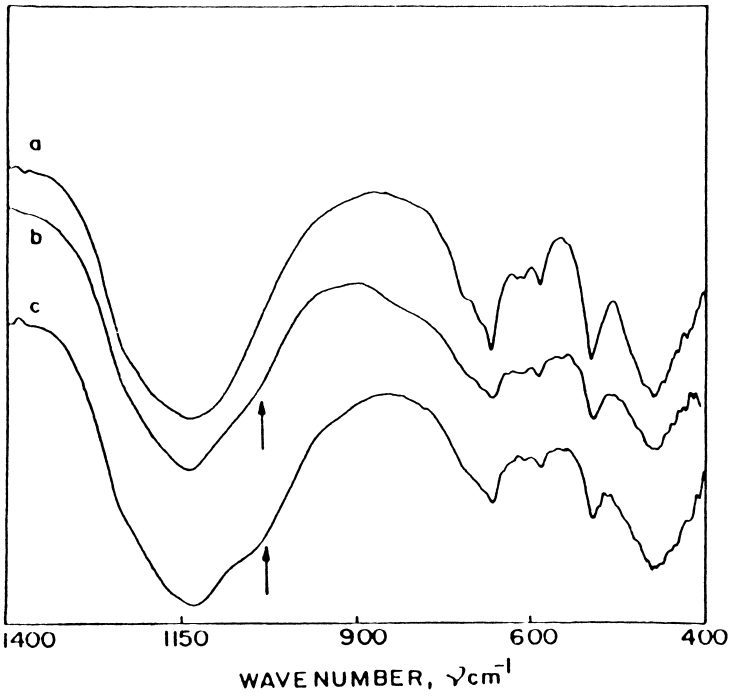

Fig. 4. Framework FTIR spectra of: (a) $AlPO_4$-5; (b) ZrAPO-5(0.04); (c) ZrAPO-5(0.08).

were observed at around 490, 562, 622 cm^{-1} due to vibrations of double ring, at 706, 732, 1042(sh) cm^{-1} due to symmetric stretching and at 1136, 1257(sh) cm^{-1} due to asymmetric stretching vibrations of AFI structure. Even though there was not much variation in the nature of the spectrum of ZrAPO-5 and pure $AlPO_4$-5, a shoulder appeared in the spectrum of ZrAPO-5 at 1042 cm^{-1} the intensity of which increased with increase in Zr content. This band was absent in the spectrum of pure $AlPO_4$-5. Similar band was also observed in the spectrum of TAPO-5 [17], which was attributed to the insertion of Ti in the framework. Therefore in the case of ZrAPO-5 also, similar conclusion may be drawn.

The FTIR spectra of surface hydroxyl groups of all samples are presented in Fig. 5(a)–(c). There were only low intensity bands at 3790, 3740 cm^{-1} and a strong band at 3680 cm^{-1} in the spectrum of $AlPO_4$-5. They are assigned to terminal Al–OH (3790, 3740) and P–OH (3680 cm^{-1}) groups on the external surface of $AlPO_4$-5. The band at 3680 cm^{-1} was observed [11,23–25] on the amorphous zirconium phosphate co-gel also, which was attributed to the isolated OH groups bonding to the surface through (i) more than one Zr cations, and (ii) a single P cation. This band was less pronounced on the surface of pure ZrO_2, wherein it is due to the bridging hydroxyl groups, Zr–(OH)–Zr. The absorption bands at 3790, 3740, 3680, 3655 and 3610 cm^{-1} were observed for ZrAPO-5 samples, (Fig. 5(b)). The additional bands at 3655 and 3610 cm^{-1} which were not found on $AlPO_4$-5 should therefore be related to the presence of Zr cations in the $AlPO_4$-5 structure. These bands cannot be due to hydroxyl groups of extra-lattice P or Al species because they were not detected in MASNMR spectroscopic studies. The intensity of these bands increased with increase in Zr content. They probably arise due to the substitution of P and P+Al pair by Zr cations in the $AlPO_4$-5 lattice, which should generate bridging hydroxyl groups Zr–(OH)–Al or Zr(Al)–(OH)–Zr.

Such bridging hydroxyl groups should be acidic and their frequency should depend on the location in the pore structure of the material. For SAPO-5 [21] these bridging hydroxyl groups (Si–OH–Al) are located in the 12-ring main channel and 8-ring side pockets.

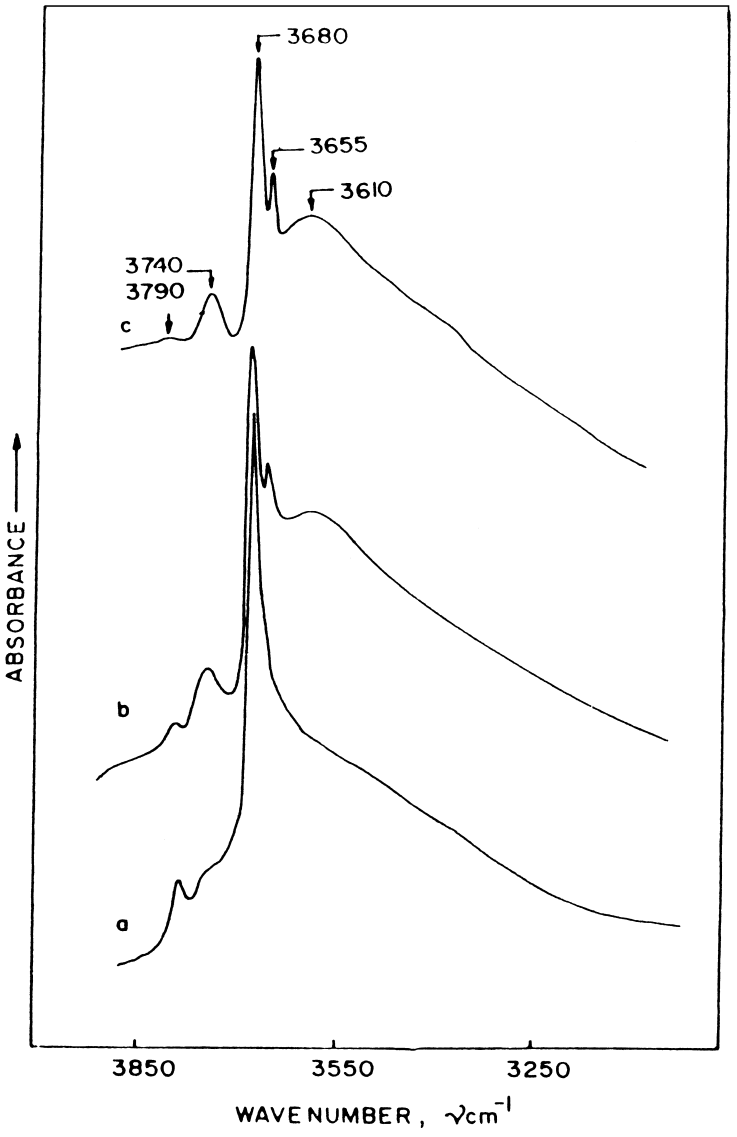

Fig. 5. FTIR spectra of surface hydroxyl groups of: (a) $AlPO_4$-5; (b) ZrAPO-5(0.04); (c) ZrAPO-5(0.08).

They give bands one at high frequency (HF) 3625 and another at low frequency (LF) at 3525 cm^{-1}. Such HF and LF bands were also observed on SAPO-37 and zeolite Y, which have duel pore structure. Therefore the bands at 3655 and 3610 cm^{-1} on ZrAPO-5 can also be assigned to such HF and LF bands similar for SAPO-5 material.

The nature of these OH groups were further studied by FTIR spectra of chemisorbed NH_3. In Fig. 6, different FTIR spectra of ZrAPO-5 sample after adsorption of NH_3 at 50°C, 100°C, 150°C, 200°C, and 250°C are presented in the range 4000–2800 cm^{-1}, which is O–H and N–H stretching mode region. The bands due to O–H stretching at 3680, 3655 and 3610 cm^{-1} appeared as negative bands and new bands due to N–H stretching of NH_4^+ actions at 3370, 3340, 3287 and 3220 cm^{-1} appear. As the chemisorbed NH_3 is desorbed at increasing temperatures,

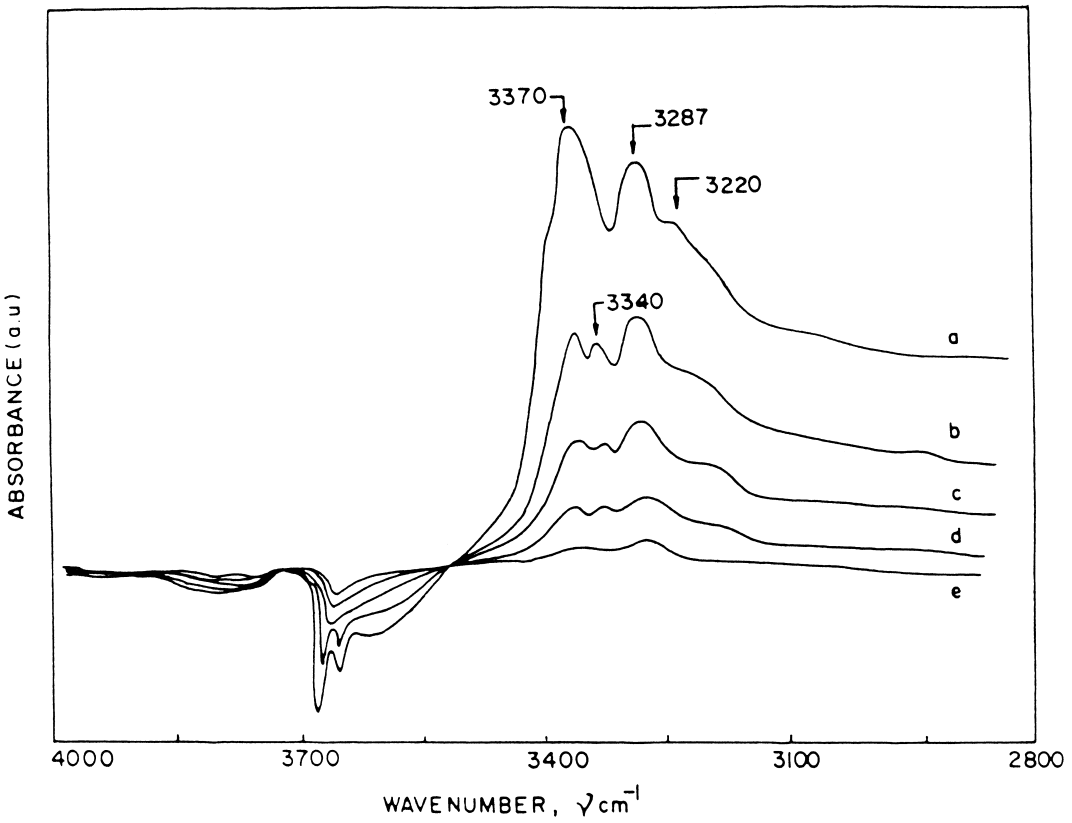

Fig. 6. FTIR difference spectra (4000–2800 cm^{-1}) of chemisorbed NH_3 on ZrAPO-5(0.08) at: (a) 50°C; (b) 100°C; (c) 150°C; (d) 200°C; (e) 250°C.

intensity of the bands at 3680, 3655 and 3610 cm^{-1} increased, while that of bands of N–H stretching decreased in intensity. Therefore the bands at 3680, 3655 and 3610 cm^{-1} are definitely due to acidic –OH groups. A clearly defined isobestic point was visible at 3513 cm^{-1}. In the case of SAPO- molecular sieves [26], the protonated NH_3 (NH_4^+ species) interact with anionic oxygen of the framework via two protons, thereby producing two different types of N–H stretching vibrations, one type belonging to free N–H bonds and another type belonging to N–H bonds involved in hydrogen bonding. The two pairs of bands at 3370, 3340 and 3287, 3220 cm^{-1} observed for ZrAPO-5 can also be ascribed to these two types of N–H stretching vibrations of adsorbed NH_3. The smaller shift to low frequencies of these bands indicate the weaker interaction between NH_4^+ protons with the framework oxygen of the acidic sites of ZrAPO-5 compared to those of SAPO-40 [26].

Fig. 7 represents difference spectra of ZrAPO-5 (0.08) sample in the region of N–H deformation vibrations. The spectra showed two bands at 1620 and 1440 cm^{-1} which decreased in intensity almost simultaneously upon increasing the sample temperature upto 250°C. Whereas in pure $AlPO_4$-5, the intensity of these bands (Fig. 7(f)–(h)) was lower and almost disappeared already at 150°C. These two bands are ascribed to co-ordinatively bound NH_3 and protonated NH_3 (NH_4^+ species) on Lewis and Brönsted acid sites of ZrAPO-5 samples, respectively.

The TPD of NH_3 curves for $AlPO_4$-5 and ZrAPO-5 are presented in Fig. 8. All the adsorbed NH_3 on $AlPO_4$-5 desorbed below 200°C, indicating the absence of strong acid sites on the surface. On the other hand, NH_3 was retained on the surface of ZrAPO-5 even upto 300°C. Therefore, we can conclude that Zr incorporation modifies the acidity of $AlPO_4$-5 making it stronger. In TAPO-5 Ulagappan et. al [17] have reported the possi-

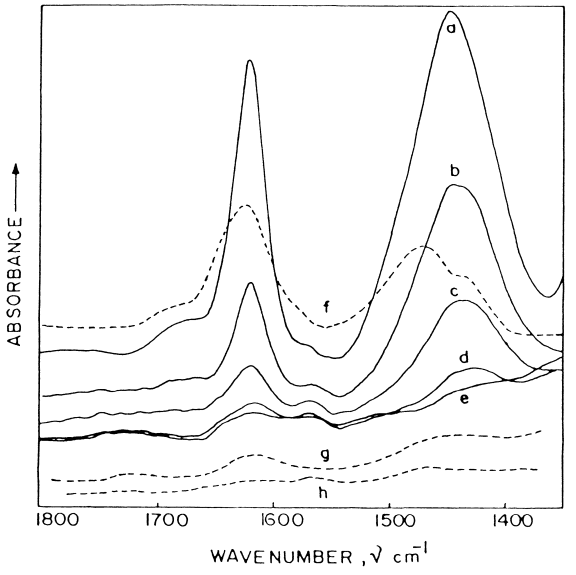

Fig. 7. FTIR difference spectra (1800–1350 cm^{-1}) of chemisorbed NH_3 on ZrAPO-5(0.08) at: (a) 50°C; (b) 100°C; (c) 150°C; (d) 200°C; (e) 250°C, on $AlPO_4$-5 at (f) 50°C; (g) 100°C; (h) 150°C.

bility of substitution of Ti for Al or P in $AlPO_4$-5 structure. Similarly, if Zr replaces some of P in $AlPO_4$-5, stronger acid sites can be generated as has been already detected by FTIR and TPD of ammonia. But if two Zr cations replace a pair of Al+P cations in the lattice, no new acidic sites can be generated.

3.1. Catalytic activity

There are many papers on catalytic activity of metal substituted AlPO-molecular sieves because of their considerable acidic properties. Studies on the catalytic activity of Zr containing molecular sieves are very few, like oxidation reactions using H_2O_2[5], toluidine isomerization [19], skeletal isomerization of linear butenes [16], nevertheless, they show that Zr incorporation in the microporous materials improves the life of the catalyst significantly. Catalytic activity of ZrAPO-5 for positional isomerization of *m*-xylene was studied as a test reaction. The reaction was carried out at 350–550°C keeping WHSV-2 h^{-1}. In Fig. 9(a), conversion of

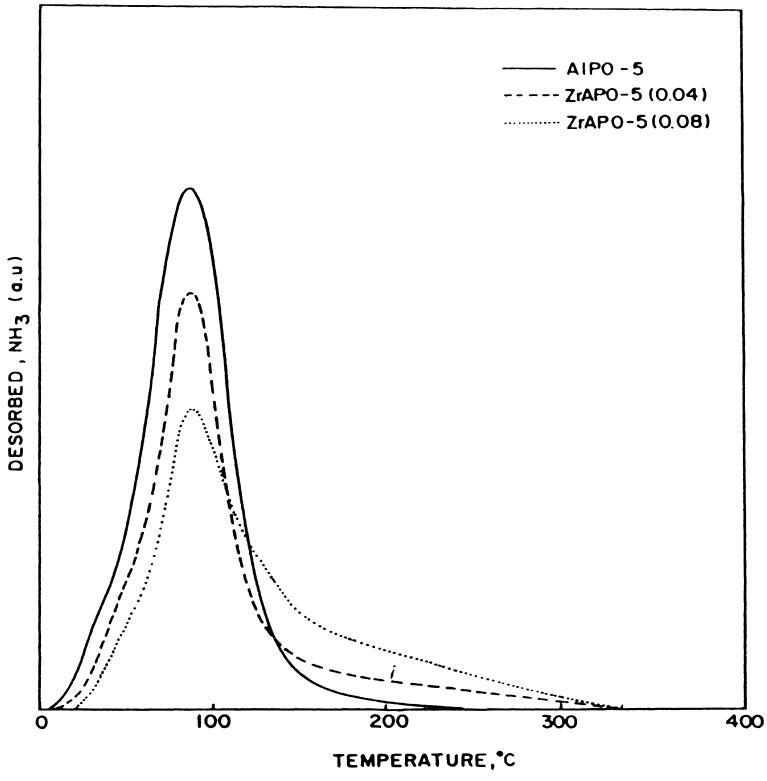

Fig. 8. TPD of NH_3 chemisorbed on: (a) $AlPO_4$-5; (b) ZrAPO-5(0.04); (c) ZrAPO-5(0.08).

m-xylene for catalysts $AlPO_4$-5, ZrAPO-5 (0.04) and ZrAPO-5 (0.08) are plotted against temperature. Increase in conversion is correlated with the zirconium content in the samples. As the zirconium substitution increased in the lattice, enhancement of acidity and activity was observed. On increasing the temperature from 500°C to 550°C, conversion increased for both ZrAPO-5 samples, whereas it decreased for $AlPO_4$-5 sample. For example, the conversion increased from 56% to 62% for ZrAPO-5 (0.08), whereas it decreased from 23% to 7% for $AlPO_4$-5. The decrease in activity may be due to the deposition of coke on the external surface blocking the pore mouth. $AlPO_4$-5 is expected to deactivate very fast similar to mordenite because of unidimensional pore system [27]. The plot of the catalytic activity with time on stream for 6 h is presented in Fig. 9(b). The stability in the reaction was found to be better for ZrAPO-5 samples as compared to $AlPO_4$-5.

In the medium pore molecular sieves, *p*-xylene is formed preferentially due to its relatively faster diffusion (10^4 times), but in case of $AlPO_4$-5 molecular sieves being the large pore variety (d=0.8 nm) the distribution of xylenes is expected to be thermodynamically controlled. In the present study, the *p*-/*o*-xylene ratio was found to be in the range 1–1.2 suggesting that there was no diffusional restriction on xylene isomers in the case of ZrAPO-5 and $AlPO_4$-5 samples.

In addition to isomerization, *m*-xylene underwent bimolecular disproportionation to form toluene and isomers of trimethylbenzene (TMB) supporting the fact that diphenyl methane type of transition state was formed during the course of the reaction. The disproportionation and isomerization activity was consistent, expected from the availability of acid sites of different strength; the isomerization occurs on the acid sites weaker than those involved in the disproportionation reactions. The estimation of the distribution of the trimethylbenzenes in products is therefore a catalytic means of probing the pore system of 12-membered ring molecular sieves [28]. Among TMBs the selectivity for 1,2,4-TMB was maximum, which can easily diffuse out from the channel compared to other TMBs.

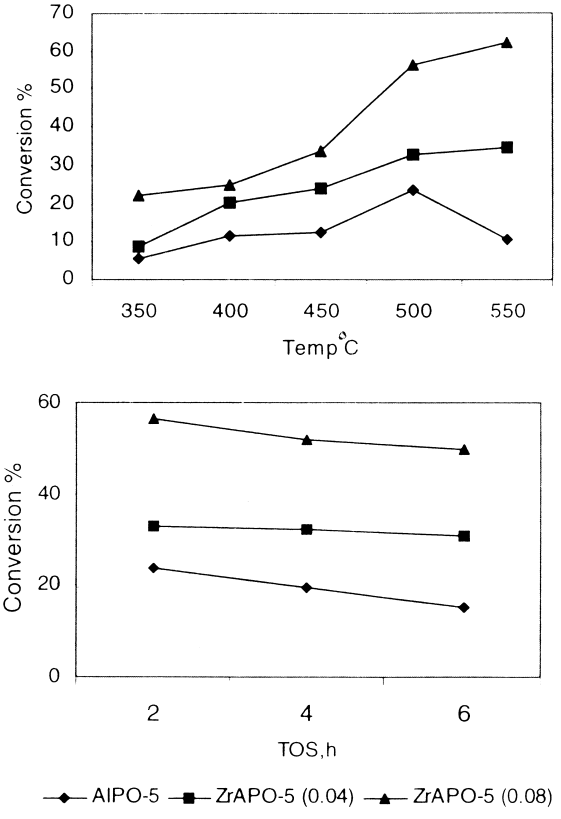

Fig. 9. Effect of (a) temperature, and (b) time on stream (at 500°C) on the conversion of *m*-xylene.

4. Conclusion

$AlPO_4$-5 and ZrAPO-5 with different Zr content have been synthesized. Physico-chemical characterization by XRD, SEM, MAS–NMR, FTIR, adsorption studies and TPD of NH_3 indicates that Zr was incorporated into the $AlPO_4$-5 structure. As a result, bridging hydroxyl groups like Zr–OH–Al and Zr(Al)–(OH)–Zr were generated. The bands at 3690, 3655 and 3610 cm^{-1} in the FTIR spectrum are attributed to bridging hydroxyl groups, which are situated in large and small pores of the structure. Brönsted and Lewis acidity of the ZrAPO-5 are higher than that of $AlPO_4$-5. Therefore ZrAPO-5 shows better catalytic activity and stability in the *m*-xylene isomerization reaction.

Acknowledgements

Authors thank Dr. A.V. Ramaswamy, Head, Catalysis Division. DPS thanks CSIR, New Delhi, for Senior Research Fellowship.

References

[1] K. Tanabe, T. Yamaguchi, Catal. Today 20 (1994) 185.
[2] T. Yamaguchi, Catal. Today 20 (1994) 199.
[3] D.A. Young, US Patents 3 329 480 and 3 329 481 (1967).
[4] H. Baltes, H. Litterer, E.I. Leupold, F. Wunder, Eur. Pat 77 523 (1983) and Ger. Offen. De. 341 285 (1983.
[5] M.K. Dongare, P. Singh, P.P. Moghe, P. Ratnasamy, Zeolites 11 (1991) 690.
[6] G. Wang, X. Wang, X. Wang, S. Yu, Stud. Surf. Sci. Catal. 83 (1993) 67.
[7] B. Rakshe, V. Ramaswamy, A.V. Ramaswamy, J. Catal 163 (1996) 501.
[8] A. Tuel, S. Gontier, R. Teissier, J. Chem. Soc. Chem. Commun (1996) 651.
[9] D.A. Ward, E.I. Ko, J. Catal 150 (1994) 18.
[10] C. Morterra, G. Cerrato, F. Pinna, M. Signaretto, G. Strukul, J. Catal 149 (1994) 181.
[11] R.A. Boyse, E.I. Ko, Catal. Lett. 38 (1996) 225.
[12] G. Alberti, M. Casciola, U. Costantino, R. Vivani, Adv. Mater. 8(4) (1996) 291.
[13] U. Ciesla, S. Schacht, G.D. Stuky, K.K. Unger, F. Schuth, Angew. Chem. Int. Ed. Engl. 35 (1996) 541.
[14] J. Kornatowski, M. Rozwadowski, W. Lutz, M. Sychev, G. Pieper, G. Finger, W.H. Baur, Zeolite science 1994: recent progress and discussions, Stud. Surf. Sci. Catal. 98 (1994) 13.
[15] J. Kornatowski, M. Sychev, G. Finger, W.H. Baur, M. Rozwadowski, Zibrowius. Proceedings of the Polish–German Zeolite Colloquium, Turun, 1992, p. 20.
[16] P. Meriaudeau, V.A. Tuan, L.N. Hung, F. Lefebvre, H.P. Nguyen, J Chem. Soc., Faraday Trans. 93(23) (1997) 4201.
[17] N. Ulagappan, V. Krishanasamy, J. Chem. Soc. Chem. Commun. (1995) 373.
[18] A. Tuel, Zeolite 15 (1995) 228.
[19] K. Eichler, E.I. Leupold, H. Arpe, H. Baltes, US Patent 4 720 583 (1988).
[20] S.G. Hegde, R.A. Abdulla, R.N. Bhat, P. Ratnasamy, Zeolite 12 (1992) 951.
[21] S.G. Hegde, P. Ratnasamy, L.M. Kustov, V.B. Kazansky, Zeolite 8 (1988) 137.
[22] D. Miller, E. John, B. Fahlke, G. Lawing, U. Haubenreisser, Zeolite 5 (1985) 53.
[23] Z. Dang, B.G. Anderson, Y. Amenomiya, B.A. Marrow, J. Phys. Chem. 99 (1995) 14437.
[24] P.A. Agron, E.L. Fuller Jr., H.F. Holmes, J. Colliod Interface Sci. 52 (1975) 553.
[25] G. Busca, V. Lorenzelli, P. Galli, A. La Gunestra, P. Patrono, J. Chem. Soc., Faraday Trans. 83 (1987) 853.
[26] B. Onida, Z. Gabelica, J. Lourenco, E. Garrone, J. Phys. Chem. 100 (1996) 11072.
[27] V.R. Choudhary, D.E. Akolekar, J. Catal. 103 (1991) 115.
[28] J. Perez-Periente, E. Sastre, V. Fornes, J.A. Martens, P.A. Jacobs, A. Corma, Appl. Catal. 69 (1991) 125.